J|A|C|S
ARTICLES
Published on Web 01/01/2003

DNA Hybridization Detection with Water-Soluble Conjugated Polymers and Chromophore-Labeled Single-Stranded DNA

Brent S. Gaylord, Alan J. Heeger, and Guillermo C. Bazan*

Contribution from the Departments of Chemistry and Materials, and Institute for Polymers and Organic Solids, University of California, Santa Barbara, California 93106

Received June 3, 2002

Abstract: A sensor is provided that detects single-stranded deoxyribonucleic acid (ssDNA) with a specific base sequence. The ssDNA sequence sensor comprises an aqueous solution containing a cationic water-soluble conjugated polymer [in this case, poly(9,9-bis(6′-*N*,*N*,*N*-trimethylammonium)-hexyl)-fluorene phenylene), **1**] with a ssDNA labeled with a dye (in this case, fluorescein). The emission of light from the sensor solution with the wavelength characteristic of the probe oligonucleotide indicates the presence of ssDNA with a specific base sequence complementary to that of the probe ssDNA-fluorescein. Maximum energy transfer from **1** to the signaling chromophore occurs when the ratio of polymer chains to DNA strands is approximately 1:1. Energy transfer from **1** results in a fluorescein emission that is more intense than that observed by direct excitation of the chromophore. Furthermore, the decrease in energy transfer upon addition of electrolyte indicates that electrostatic forces dominate the interactions between **1** and DNA.

Introduction

The value of DNA hybridization detection in real time and with high sensitivity is well appreciated for scientific and economic reasons.[1] It can be used for a variety of applications, including medical diagnostics, identification of genetic mutations, and monitoring of gene delivery.[2] Several innovative assays have been reported recently, including DNA microarray technology, which relies on the hybridization between DNA sequences on a microarray surface,[3] the use of semiconductor crystals or quantum dots as fluorescent probes,[4−6] detection methods based on nanoparticle-ampilified surface plasmon resonance,[7−9] and the use of redox-active nucleic acids.[10] Homogeneous fluorescence analysis, although established for some time,[11] remains of paramount importance, principally because of its high sensitivity and ease of operation.[12] Fluorescence methods based on cationic organic dyes such as ethidium bromide and thiazole orange, which are only emissive when intercalated into the grooves of double-stranded DNA (dsDNA), serve as direct DNA hybridization probes, but lack sequence specificity.[13,14] Energy/electron transfer pairs, developed for strand-specific assays, require labeling of two nucleic acids or dual modification of the same altered strand (*i.e.*, molecular beacons) and have shown the ability to detect unamplified DNA based on dual-probe detection.[15,16] The difficulty in labeling two DNA sites gives rise to low yields and singly labeled impurities, which lower sensitivity.[17] Much of the motivation behind these studies is to develop simple, economic methods for evaluating specific hybridization with minimal DNA modifications.

In response to the motivations listed above, we recently reported a DNA sensor assay that relies on the light harvesting and electrostatic properties of cationic conjugated polymers (CPs).[18,19] The strand-specific assay is illustrated in Scheme 1. One begins with a solution that contains a CP (shown in black) and a peptide nucleic acid (PNA) strand[20] (shown in blue) labeled with a chromophore dye (C*). The optical properties of the CP and C* are optimized so that Förster energy transfer (FRET) from CP

* Corresponding author. E-mail: Bazan@chem.ucsb.edu.

(1) (a) Wang, J. *Nucleic Acids Res.* **2000**, *28*, 3011. (b) Umek, R. M.; Lin, S. W.; Vielmetter, J.; Terbrueggen, R. H.; Irvine, B.; Yu, C. J.; Kayyem, J. F.; Yowanto, H.; Blackburn, G. F.; Farkas, D. H.; Chen, Y. P. *J. Mol. Diag.* **2001**, *3*, 74. (c) Schork, N. J.; Fallin, D.; Lanchbury, J. S. *Clin. Genet.* **2000**, *58*, 250.
(2) (a) Balakin, K. V.; Korshun, V. A.; Mikhalev, I. I.; Maleev, G. V.; Malakhov A. D.; Prokhorenko, I. A.; Berlin, Yu. A. *Biosens. Bioelectron.* **1998**, *13*, 771.
(3) Niemeyer, C. M.; Blohm, D. *Angew. Chem., Int. Ed.* **1999**, *38*, 2865.
(4) Gerion, D.; Parak, W. J.; Williams, S. C.; Zanchet, D.; Micheel, C. M.; Alivisatos, A. P. *J. Am. Chem. Soc.* **2002**, *124*, 7070.
(5) Bruchez, M.; Moronne, M.; Gin, P.; Weiss, S.; Alivisatos, A. P. *Science* **1998**, *281*, 2013.
(6) Chan, W. C. W.; Nie S. M. *Science* **1998**, *281*, 2016.
(7) He, L.; Musick, M. D.; Nicewarner, S. R.; Salinas, F. G.; Benkovic, S. J.; Natan, M. J.; Keating, C. D. *J. Am. Chem. Soc.* **2000**, *122*, 9071.
(8) Nelson, B. P.; Grimsrud, T. E.; Liles, M. R.; Goodman, R. M.; Corn, R. M. *Anal. Chem.* **2001**, *73*, 1.
(9) Tombelli, S.; Minunni, M.; Mascini, M. *Anal. Lett.* **2002**, *35*, 599.
(10) Patolsky, F.; Weizmann, Y.; Willner, I. *J. Am. Chem. Soc.* **2002**, *124*, 770. (b) Caruana, D. J.; Hellerr. A. *J. Am. Chem. Soc.* **1999**, *121*, 769.
(11) Sueda, S.; Yuan, J.; Matsumoto, K. *Bioconjugate Chem.* **2002**, *13*, 200 and the references therein.
(12) Paris, P. L.; Langenhan, J. M.; Kool, E. T. *Nucleic Acids Res.* **1998**, *26*, 3789.
(13) LePecq, J. B.; Paoletti, C. *J. Mol. Biol.* **1967**, *27*, 87.
(14) Petty, J. T.; Bordelon, J. A.; Robertson, M. E. *J. Phys. Chem. B* **2000**, *104*, 7221.
(15) Cardullo, R. A.; Agrawal, S.; Flores, C.; Zamechnik, P. C.; Wolf, D. E. *Proc. Natl. Acad. Sci. U.S.A.* **1988**, *85*, 8790.
(16) Castro, A.; Williams, J. G. K. *Anal. Chem.* **1997**, *69*, 3915.
(17) Knemeyer, J.; Marme, N.; Sauer, M. *Anal. Chem.* **2000**, *72*, 3717.
(18) Gaylord, B. S.; Heeger, A. J.; Bazan, G. C. *Proc. Natl. Acad. Sci. U.S.A.* **2002**, *99*, 10954.
(19) For the use of conjugated polymer in biosensor applications see: (a) Chen, L.; Mcbranch, D. W.; Wang, H. L.; Helgeson, R.; Wudl, F.; Whitten, D. G. *Proc. Natl. Acad. Sci. U.S.A.* **2000**, *96*, 12287. (b) Wang, D.; Gong, X.; Heeger, P. S.; Rininsland, F.; Bazan, G. C.; Heeger, A. J. *Proc. Natl. Acad. Sci. U.S.A.* **2002**, *99*, 49. (c) Ho, H.-A.; Boissinot, M.; Bergeron, M. G.; Corbeil, G.; Dore, K.; Boudreau, D.; Leclerc, M. *Angew. Chem., Int. Ed.* **2002**, *41*, 1548.

10.1021/ja027152+ CCC: $25.00

Scheme 1

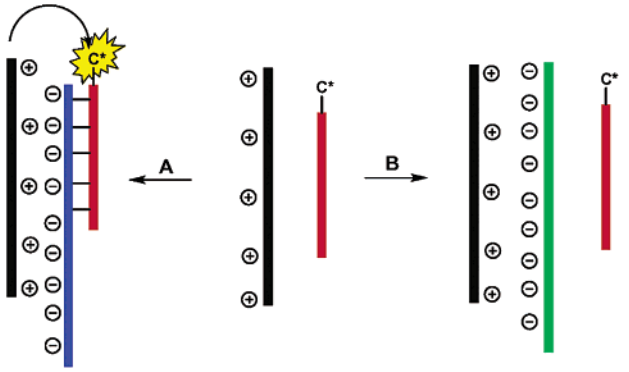

(donor) to C* (acceptor) is favored.[21] Because PNA is neutral, there are no electrostatic interactions between PNA-C* and the CP. Consider next the interaction between PNA and a single-stranded DNA (ssDNA). Situation **A** corresponds with addition of a complementary ssDNA (shown in blue), which hybridizes with the target PNA. Hybridization endows the C*-bearing macromolecule with multiple negative charges. Electrostatic attraction causes the formation of a complex between CP and the DNA/PNA-C* hybrid, allowing for FRET. When a ssDNA is added that does not match the PNA sequence (shown in green), situation **B**, hybridization does not take place. Electrostatic complexation occurs only between the CP and DNA. The distance between CP and PNA-C* is too large for FRET. Scheme 1 is general; the number of charges between CP and DNA/PNA-C* may or may not be the same and the length of the PNA-C* probe may or may not be of the same length as the target sequence.

Scheme 1 was designed to take advantage of the optical amplification of conjugated polymers[22] and interactions typical of polyelectrolytes. In a CP, for which the chain length is larger than the conjugation length, the backbone serves to hold a series of conjugated segments in close proximity. Exciton migration to low-energy sites along the chain gives rise to exceptionally high-fluorescence quenching efficiencies.[23,24] Water solublity of the CPs is required, and this property is typically achieved by attachment of charged groups pendant to the main chain.[25] The resulting properties in water are typical of amphiphilic polyelectrolytes, for

(20) In PNAs, the negatively charged phosphate linkages in DNA are replaced with peptomimetic neutral amide linkages. PNA/DNA complexes form more quickly, with higher binding energies, and they are more specific than analogous DNA/DNA complexes. These enhanced properties result from the absence of the Coulomb repulsion between negatively charged DNA strands. PNA complexes are thus more thermally stable and, by virtue of their backbone, less susceptible to biological degradation by nucleases, proteases, and peptidases. Additionally, their general insensitivity to ionic strength and pH during hybridization provides a wider platform for DNA detection. For references see: (a) Nielsen, P. E.; Egholm, M. *Peptide Nucleic Acids: Protocols and Applications*; Horizon Scientific Press: Portland, 1999. (b) Stender, H.; Fiandaca, M.; Hyldig-Nielsen, J. J.; Coull, J. *J. Microbiol. Methods* **2002**, *48*, 1. (c) Egholm, M.; Buchardt, O.; Christensen, L.; Behrens, C.; Freier, S. M.; Driver, D. A.; Berg, R. H.; Kim, S. K.; Norden, B.; Nielsen, P. E. *Nature* **1993**, *365*, 556. (d) Nielsen, P. E. *Curr. Opin. Biotechnol.* **1999**, *10*, 71. (e) Demidov, V. V. *Biochem. Pharmacol.* **1994**, *48*, 1310.

(21) Lakowicz, J. R. *Principles of Fluorescence Spectroscopy*; Kluwer Academic/Plenum Publishers: New York, 1999.

(22) (a) McQuade, D. T.; Pullen. A. E.; Swager, T. M. *Chem. Rev.* **2000**, *100*, 2537. (b) McQuade, D. T.; Hegedus, A. H.; Swager, T. M. *J. Am. Chem. Soc.* **2000**, *122*, 12389. (c) Yang, J. S.; Swager, T. M. *J. Am. Chem. Soc.* **1998**, *120*, 11864. (d) Harrison, B. S.; Ramey, M. B.; Reynolds, J. R. *J. Am. Chem. Soc.* **2000**, *122*, 8561.

(23) Wang, J.; Wang, D.; Miller, E. K.; Moses, D.; Bazan, G. C.; Heeger, A. J. *Macromolecules* **2000**, *33*, 5153.

(24) Gaylord, B. S.; Wang, S.; Heeger, A. J.; Bazan, G. C. *J. Am. Chem. Soc.* **2001**, *123*, 6417.

(25) Shi, S. Q.; Wudl, F. *Macromolecules* **1990**, *23*, 2119.

(26) Kabanov, A. V., Felgner, P., Seymour, L. W., Eds. *Self-assembling Complexes for Gene Delivery. From Laborotary to Clinical Trial*; John Wiley: Chichester, 1998.

Scheme 2

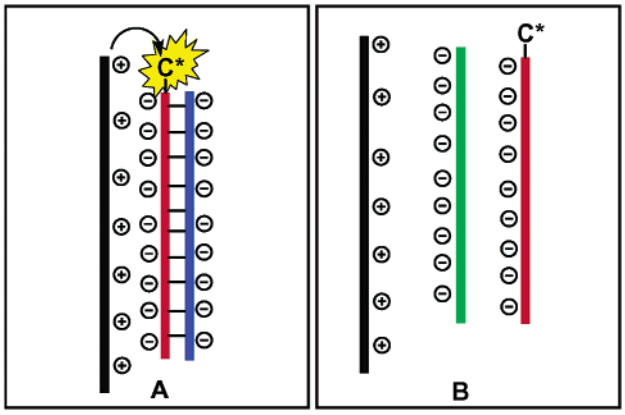

which interactions with DNA have been studied.[26] Indeed, the strength of the interactions between cationic polyelectrolytes and DNA has recently been used to recognize the tertiary structure of plasmid DNA.[27]

It would be highly desirable to modify the process in Scheme 1 to take advantage of C*-labeled ssDNA as the optical reporter. Although PNA is widely used, the synthesis and purification of labeled DNA is more straightforward. DNA/DNA interactions are much more common in biology and are therefore better catalogued and understood. In this contribution, we show that, indeed, Scheme 1 can be adapted to use ssDNA-C* as the optical probe for the presence of a specified DNA sequence.

Results and Discussion

The modification of Scheme 1 was based on the idea that, given a set number of repeat units, the electrostatic interaction between a dsDNA and a cationic CP would be stronger than that of a ssDNA and the CP. Scheme 2 shows the two situations resulting from the interaction between ssDNA-C* (shown in red) and a complementary strand (in blue, situation A) or a noncomplementary strand (in green, situation B), when in the presence of a cationic CP (in black). The higher local charge density of the double strand should result in a stronger dsDNA-C*/CP electrostatic attraction, relative to ssDNA-C*/CP.[28] Additionally, in the case of a noncomplementary sequence, the nonhybridized strand will interfere with the ssDNA-C*/CP interactions. Based exclusively on these considerations, one would expect closer proximity when the "target" strand is present and therefore more efficient FRET from the CP to C* in situation A.

Energy transfer experiments and hybridization tests used poly-(9,9-bis(6′-*N*,*N*,*N*-trimethylammonium)-hexyl)-fluorene phenylene) (**1**). The synthesis and photophysics of **1** have recently been reported.[29] To examine the feasibility of Scheme 2, we chose the specific probe sequence **2**, corresponding to a segment of the anthrax

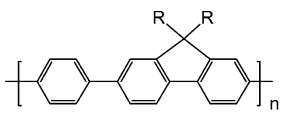

1 -R = -$(CH_2)_6NMe_3^{\oplus}$ $I^{\ominus}$

2-C*: 5′-FI-GTAAATGGTGTTAGGGTTGC-3′
3: 5′-GCAACCCTAACACCATTTAC-3′
4: 5′-GACTCAATGGCGTTAGACTG-3′
5: 5′-CATCTGTAAATCCAAGAGTAGCAACCCTAACACCATTTAC-3′
6: 5′-AAAATATTGTGTATCAAAATGTAAATGGTGTTAGGGTTGC-3′

(*Bacillus anthracis*) spore encapsulation plasmid, pX02, with fluorescein as C*.[30,31]

The absorption and emission spectra of **1** and **2**-C* in Figure 1 show an optical window for selective excitation of **1**, between the

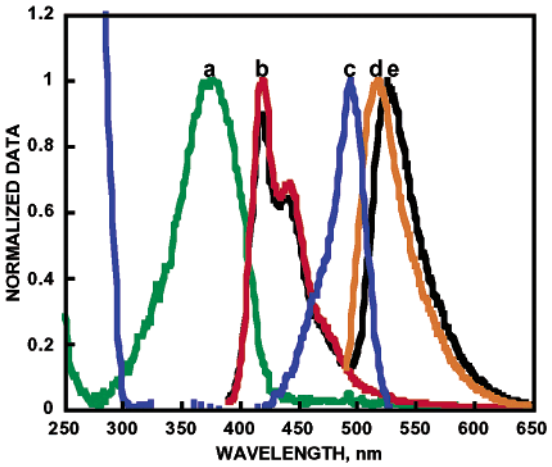

Figure 1. Absorption [(a) green and (c) blue] and emission [(b) red and (d) orange] spectra of polymer **1** [(a) and (b)] and ssDNA probe **2** [(c) and (d)] upon excitation at 380 and 480 nm, respectively. The emission of the energy-transfer complex [(e) black] excited at 380 nm is also shown ([**1**] = 8.41×10^{-7} M, [**2**-C*] = 2.1×10^{-8} M).

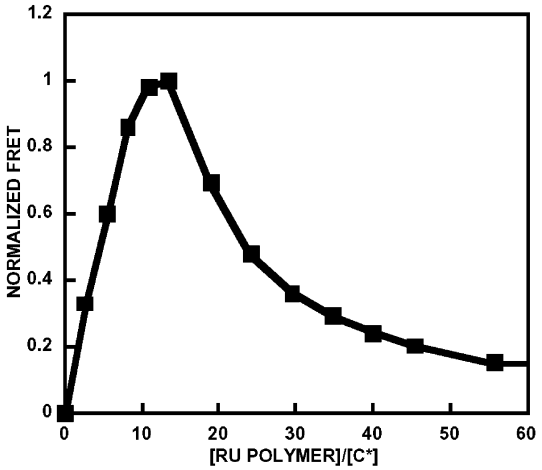

Figure 2. FRET ratio as a function of [RU]/[**2**-C*], where RU corresponds to the polymer repeat unit. The concentration of **2**-C* was kept constant at 2.1×10^{-8} M. Fluorescence was measured by excitation at 380 nm. Measurements were performed in SSC buffer.

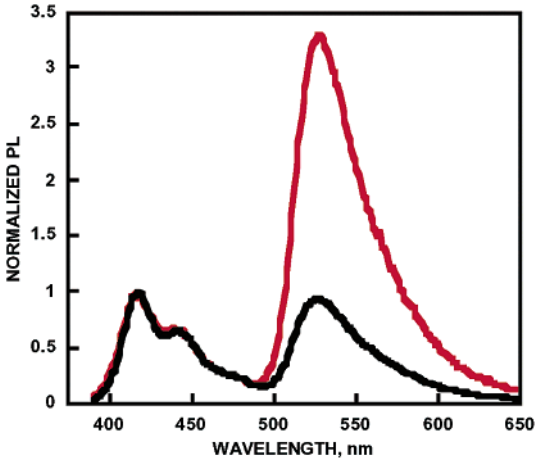

Figure 3. Emission spectra of **1** with hybridized (**2**-C*/**3**, red) and nonhybridized (**2**-C* and **4**, black) DNA probes in SSC buffer. The spectra were normalized to polymer emission.

DNA and C* absorption. Furthermore, the emission of **1** overlaps the absorption of C*, an important condition for FRET.[21] Indeed, in a solution of **1** and **2**-C* excitation of **1** at 380 nm results in efficient FRET to C* (Figure 1). We evaluate the FRET efficiency by the ratio of integrated acceptor to donor emission. Note also that there is a 10 nm shift in the C* emission in the presence of **1**, consistent with an increase in polarity in the vicinity of C* by the close proximity to **1**.

FRET optimization involved varying the donor to acceptor ratio. These measurements were done in 100 mM NaCl and 10 mM sodium citrate at pH = 8.3 (SSC buffer). At a concentration of [**2**-C*] = 2.1×10^{-8} M, the initial additions of polymer caused an immediate rise in the FRET ratio, followed by a concomitant drop as donor concentrations far exceed that of the acceptor (Figure 2). The maximum FRET ratio corresponds to a near 1:1 ratio of polymer chains to DNA strands, according to previously published molecular weight information.[29] At high [**1**] not every polymer chain can be tightly complexed to ssDNA-C*, and the donor emission rises faster than that of C*. Once the repeat unit of polymer to DNA probe reaches approximately 100 the photoluminescence of the C* no longer increases, indicating acceptor saturation. At the saturation point, the integrated C* emission was ~4 fold greater than that observed from the directly excited (480 nm) probe in the absence of **1**, indicating signal amplification by the conjugated polymer. An additional ssDNA probe with a different base pair sequence provided similar results to that of **2**, with the optimum FRET at a 1:1 ratio of polymer chains to DNA strands (see Supporting Information).

The probe **2**-C* was annealed at 2 °C below its T_m (58.4 °C) in the presence of an equal molar amount of its 20 base pair complementary strand, **3**, and in an identical fashion with a noncomplementary 20 base pair strand, **4**. The resulting solutions were mixed with **1**. A direct comparison of the fluorescence (λ_{exc} = 380 nm) with [**2**-C*] = 2.1×10^{-8} M and [**1**] = 5.1×10^{-7} M (Figure 3) revealed ~3 fold higher FRET ratio for the hybridized DNA. The differences in FRET are attributed to a closer proximity between C* and **1**, as shown in Scheme 2. Examination of the **2**-C*/**3** hybrid with increasing [**1**] also indicated a maximum FRET ratio at approximately 1:1 polymer chains to dsDNA strands. The data in Figure 3 show that situation **A** in Scheme 2 indeed leads to higher FRET ratios and that CPs can be used to monitor the presence of a complementary strand to ssDNA-C*.

A different 20 base pair probe sequence was also selected from the same Anthrax encapsulation gene for further testing. Differences between hybridized and nonhybridized strands in this case yielded FRET differences similar to those shown in Figure 3 (Supporting Information).

It is also highly significant that these optical differences are observed in the presence of a 10 mM sodium citrate and 100 mM sodium chloride buffer. Buffer ions screen negative charges on complementary DNA, which facilitates hybridization but weakens electrostatic interactions between CPs and fluorescence quenchers

(27) Bronich, T. K.; Nguyen, H. K.; Eisenberg, A.; Kabanov, A. V. *J. Am. Chem. Soc.* **2000**, *122*, 8339.
(28) (a) Pullman, B.; Lavery, R.; Pullman, A. *Eur. J. Biochem.* **1982**, *124*, 229. (b) Minehan, D. S.; Marx, D. A.; Tripathy, S. K. *Macromolecules* **1994**, *27*, 777.
(29) Stork, M. S.; Gaylord, B. S.; Heeger, A. J.; Bazan, G. C. *Adv. Mater.* **2002**, *14*, 361.
(30) Makino, S.; Uchida, I.; Terakado, N.; Sasakawa, C.; Yoshikawa, M. *J. Bacteriol.* **1989**, *171*, 722.
(31) Fluorescein was chosen because it is one of the most ubiquitous dyes used in FRET experiments and because it can be easily attached to DNA structures. Its fluorescence and absorbance properties are known to be pH dependent, and the highest quantum yield is obtained for the fluorescein dianion. The pH of the SSC buffer used for this study is about 8.3. In our experiment, the quantum yield of ss-DNA-C* was determined to be 94%, using 9,10-diphenylanthraacene as the standard.

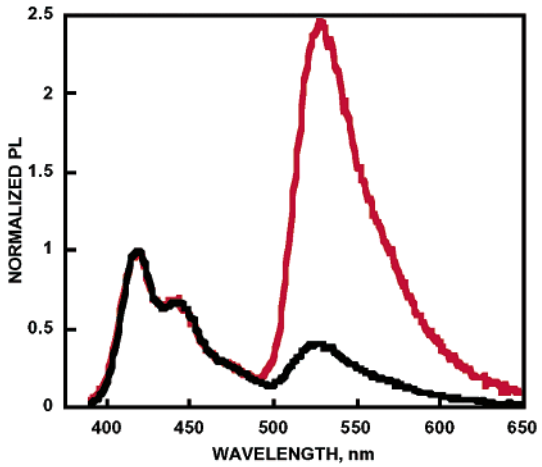

Figure 4. Emission spectra of **1** with hybridized (**2**-C*/**5**, red) and nonhybridized (**2**-C* and **6**, black) DNA probes in SSC buffer. The spectra were normalized to polymer emission.

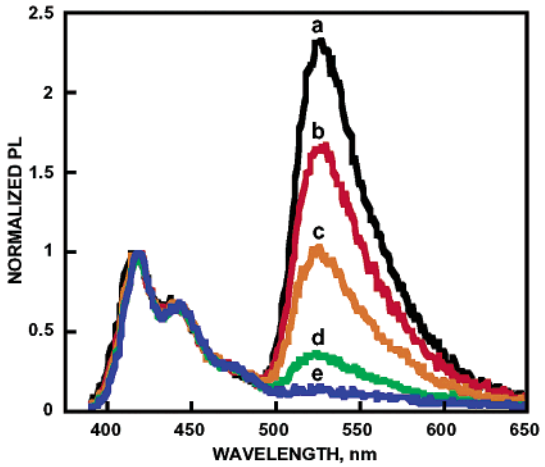

Figure 5. Result of increased [NaCl] on the energy transfer between hybridized **2**-C*/**5** and **1**. The concentration of NaCl ranges from the initial buffer concentration (0.100 M NaCl and 0.010 NaCitrate) to 1.238 M, with $a = 0.110$ M, $b = 0.316$ M, $c = 0.397$ M, $d = 0.597$ M and $e = 1.238$ M.

of opposite charge.[32] Multiple charge interactions between **1** and the DNA molecules are capable of compensating for this screening effect.

Many current detection platforms such as TaqMan and Molecular Beacons use short oligonucleotide probes to identify longer DNA sequences of interest.[33] To further evaluate the effectiveness of Scheme 2 we examined the effect of longer target sequences. For this test equal molar amounts of the 20 base pair **2**-C* were mixed with either its complementary or noncomplementary sequence, strands **5** and **6**, respectively (both 40 base pairs in length). As shown in Figure 4 ($[\mathbf{1}] = 2.8 \times 10^{-7}$ M and $[\mathbf{2}{-}\mathrm{C}^*] = 2.1 \times 10^{-8}$ M), one again observes a larger FRET ratio when the complementary sequence is used. Dilution of this same system in SSC buffer still provided energy transfer (ET) ratios for the complementary sequence that were over 3 times higher at [**2**-C*] < 30 nM than did the noncomplementary sequence, using a standard fluorometer. Comparison of Figures 3 and 4 reveals smaller FRET ratios with this longer target sequence. We suspect that the larger DNA structure presents more sites (or volume) for complexation with **1**, increasing the average distance between C* and the conjugated polymer backbone.

As stated previously, buffered solutions are used to aid DNA hybridization by minimizing the electrostatic repulsion between like charged strands. The Coulombic potential between charged surfaces of low potential is often approximated using the Debye−Hückel equation:

$$\psi_x \approx \psi_o e^{-\kappa x} \tag{1}$$

where ψ_o is the surface potential and $1/\kappa$ represents the characteristic Debye length. The Debye length in aqueous solutions can be determined by the Grahame equation which, simplified for 1:1 electrolyte solutions such as NaCl, is given as[32]

$$\frac{1}{\kappa} = \frac{0.304}{\sqrt{[\mathrm{NaCl}]}}\ \mathrm{nm}. \tag{2}$$

Increasing the concentration of NaCl thus decreases, or collapses, the electrostatic layer of counterions resulting in an exponential decrease in the potential between two surfaces. This is often referred to as electrostatic screening.

According to the Debye−Hückel theory, if the concentration of NaCl in the buffer increases, the attraction between the oppositely charged polymers should decrease and result in a drop in the energy transfer between **2**-C* and **1**. In buffer (0.11 M salt) the electrostatic potential between the hybridized DNA ($[\mathbf{2}\text{-C}^*/\mathbf{5}] = 2.1 \times 10^{-8}$ M) and **1** (2.1×10^{-7} M) is sufficiently strong to bring the two together as seen in Figures 4 and 5. Subsequent increases in the concentration of NaCl result in a FRET decrease, as shown in Figure 5.

The results in Figure 5 confirm the importance of electrostatic interactions in determining the success of Scheme 2. Förster energy transfer has a $1/r^6$ distance dependence, thus as the DNA and **1** begin to dissociate (increasing the average distance) because of the weaker electrostatic potential between the oppositely charged macromolecules, the amount of energy transfer will drop. At an ionic strength of 1.238 M, **1** was nearly completely screened from the DNA. This evidence suggests that the dominant interaction between **1** and DNA is electrostatic in nature.[34] Experiments also done on the noncomplementary DNA (strands **2**-C* and **6**) in an identical fashion yield a similar loss of energy transfer with increasing ionic strength (Supporting Information).

Conclusion

In summary, it is possible to use the optical amplification of cationic conjugated polymers to detect hybridization to a singly labeled oligonucleotide strand. This method provides a homogeneous assay that takes advantage of fluorescence detection methods, it eliminates the need for multiple probes and complex DNA structures, and it circumvents the need to use labeled PNA, as in Scheme 1. Excitation of the conjugated polymers results in larger signal amplification, relative to commonly used small molecules. The set of experiments shown in Figure 5 demonstrates the role of electrostatic forces in controlling the average distance between the conjugated polymer and the chromophore. Further optimization of CP structure/optical properties, with a better understanding of the

(32) Israelachvili, J. *Intermolecular & Surface Forces*; Academic Press: London, 1992.

(33) (a) Giesendorf, B. A. J.; Vet, J. A. M.; Tyangi, S.; Mensink, E. J. M. G.; Trijbels, F. J. M.; Blom, H. J. *Clin. Chem.* **1998**, *44*, 482. (b) Giulietti, A.; Overbergh, L.; Valckx, D.; Decallonne, B.; Bouillon, R.; Mathieu, C. *Methods* **2001**, *25*, 386.

(34) Circular dichroism experiments indicated no change in DNA conformation upon addition of **1**, nor did they show the emergence of any signal from **1**. This result indicates that the rigid polyfluorene structure most likely does not adapt to the DNA conformation upon complexation. They also suggest that binding into the grooves of DNA, like other cationic dyes such as ethidium bromide, is not a dominant form of association. Any twisting to accommodate such groove binding or helical conformation would likely shorten the effective conjugation length in the conducting polymer and thus blue shift the emission. This information strengthens the idea that interactions between DNA and **1** are largely due to electrostatics.

forces that control the association between conjugated polyelectrolytes and DNA should yield practical detection platforms. Current studies in our laboratories are geared toward deconvoluting the contribution of electrostatic forces from that of hydrophobic interactions not accounted for in the two situations shown in Scheme 2.[35] Additional work is also being done to examine how sequence, chain/charge screening, acceptor environment, and electrostatic differences affect ET processes between conjugated polymers and DNA.

Experimental Section

General Details. Samples were prepared by initially determining the DNA concentrations using 260 nm absorbance measurements in 200 μL samples. Once the ssDNA concentrations were known, equal molar amounts of target DNA (complementary or noncomplementary) were mixed with the labeled probe sequence **2-**C*. Both complementary and noncomplementary samples were annealed at 2 °C below the proper T_m for 20 min and were then allowed to slowly cool to room temperature. Hybridization was verified by melting a sample while monitoring the absorbance signal at 260 nm. DNA concentrations and melting profiles were measured using a Perkin−Elmer DU600 UV/visible spectrophotometer. Energy transfer was measured using 3 mL samples of both complementary and noncomplementary DNA at a fixed concentration. Successive additions of CP were done to determine optimum ratios of ET. Samples were placed in a vortex apparatus (Scientific Industries Vortex 2-Genie) between each fluorescence measurement (after each addition of polymer) to mix the components well. Fluorescence intensities were determined as the integrated area of the emission spectra, and FRET ratios were calculated as the area of the donor (CP) over the area of the acceptor (C*). All fluorescence and energy-transfer measurements were done using a PTI Quantum Master fluorometer equipped with a xenon lamp excitation source and a Hamamatsu 928 PMT. DNA strands were used as received from Sigma Genosys. The citrate buffer contained 100 mM sodium chloride and 10 mM sodium citrate at pH 8.3. The water used was purified using a Millipore filtration system.

(35) Hydrophobic interactions between aromatic polymer units and DNA bases have also been recognized. See for example: Ganachaud, F.; Elaïssari, A.; Pichot, C.; Laayoun, A.; Cros, P. *Langmuir* **1997**, *13*, 701.

Acknowledgment. Financial support from the National Science Foundation (DMR 0097611) and the Office of Naval Research is gratefully acknowledged.

Supporting Information Available: Additional FRET experiments with different DNA sequences (PDF). The material is available free of charge via the Internet at http://pubs.acs.org.

JA027152+